Biochemical Engineering

James M. Lee

Department of Chemical Engineering
Washington State University
Pullman, WA 99164-2714
jmlee@wsu.edu

Last Update: August 10, 2001

This book was originally published by Prentice-Hall Inc. in 1992.

Chapter 9

Agitation and Aeration

9.1. Introduction

One of the most important factors to consider in designing a fermenter is the provision for adequate mixing of its contents. The main objectives of mixing in fermentation are to disperse the air bubbles, to suspend the microorganisms (or animal and plant tissues), and to enhance heat and mass transfer in the medium.

Since most nutrients are highly soluble in water, very little mixing is required during fermentation just to mix the medium as microorganisms consume nutrients. However, dissolved oxygen in the medium is an exception because its solubility in a fermentation medium is very low, while its demand for the growth of aerobic microorganisms is high.

For example, when the oxygen is provided from air, the typical maximum concentration of oxygen in aqueous solution is on the order of 6 to 8 mg/L. Oxygen requirement of cells is, although it can vary widely depending on microorganisms, on the order of 1 g/L h. Even though a fermentation medium is fully saturated with oxygen, the dissolved oxygen will be consumed in less than one minute by organisms if not provided continuously. Adequate oxygen supply to cells is often critical in aerobic fermentation. Even temporary depletion of oxygen can damage cells irreversibly. Therefore, gaseous oxygen must be supplied continuously to meet the requirements for high oxygen needs of microorganisms, and the oxygen transfer can be a major limiting step for cell growth and metabolism.

Mixing provided by a laboratory shaker apparatus is adequate to cultivate microorganisms in flasks or test tubes. Rotary or reciprocating action of a shaker is effective to provide gentle mixing and surface aeration. For bench-, pilot-, and production-scale fermenters, the mixing is usually provided by mechanical agitation with or without aeration. The most widely used arrangement is the radial-flow impeller with six flat blades mounted on a disk (Figure 9.1), which is called flat-blade disk turbine or Rushton turbine.

Radial-flow impellers (paddles and turbines) produce flow radially from the turbine blades toward the side of the vessel, where the flow splits into two directions: one part goes upward along the side, back to the center along the liquid surface, and down to the impeller region along the agitating shaft; and the other goes downward along the side and bottom, then back to the impeller region. On the other hand, the axial flow impellers (propellers and pitched blade paddles) generate flow downward to the tank bottom, then up the side and back down the center to the impeller region. Therefore, the flat-blade disk turbine has the advantage of limiting the short-circuiting of gas along the drive shaft by forcing the gas, introduced from below, along the path into the discharge jet.

Mass-Transfer Path: The path of gaseous substrate from a gas bubble to an organelle in a microorganism can be divided into several steps (Figure 9.2) as follows:

1. Transfer from bulk gas in a bubble to a relatively unmixed gas layer
2. Diffusion through the relatively unmixed gas layer
3. Diffusion through the relatively unmixed liquid layer surrounding the bubble
4. Transfer from the relatively unmixed liquid layer to the bulk liquid
5. Transfer from the bulk liquid to the relatively unmixed liquid layer surrounding a microorganism
6. Diffusion through the relatively unmixed liquid layer
7. Diffusion from the surface of a microorganism to an organelle in which oxygen is consumed

Steps 3 and 5, the diffusion through the relatively unmixed liquid layers of the bubble and the microorganism, are the slowest among those outlined previously and, as a result, control the overall mass-transfer rate. Agitation and aeration enhance the rate of mass transfer in these steps and increase the interfacial area of both gas and liquid.

In this chapter, we study various correlations for gas-liquid mass transfer, interfacial area, bubble size, gas hold-up, agitation power consumption, and volumetric mass-transfer coefficient, which are vital tools for the design and operation of fermenter systems. Criteria for the scale-up and shear sensitive mixing are also presented. First of all, let's review basic mass-transfer concepts important in understanding gas-liquid mass transfer in a fermentation system.

9.2. Basic Mass-Transfer Concepts

9.2.1. Molecular Diffusion in Liquids

When the concentration of a component varies from one point to another, the component has a tendency to flow in the direction that will reduce the local differences in concentration.

Molar flux of a component A relative to the average molal velocity of all constituent J_A is proportional to the concentration gradient dC_A/dz as

$$J_A = -D_{AB}\frac{dC_A}{dz} \tag{9.1}$$

which is Fick's first law written for the z-direction. The D_{AB} in Eq. (9.1) is the diffusivity of component A through B, which is a measure of its diffusive mobility.

Molar flux relative to stationary coordinate N_A is equal to

$$N_A = \frac{C_A}{C}(N_A + N_B) - D_{AB}\frac{dC_A}{dz} \tag{9.2}$$

where C is total concentration of components A and B and N_B is the molar flux of B relative to stationary coordinate. The first term of the right hand side of Eq. (9.2) is the flux due to bulk flow, and the second term is due to the diffusion. For dilute solution of A,

$$N_A \approx J_A \tag{9.3}$$

Diffusivity: The kinetic theory of liquids is much less advanced than that of gases. Therefore, the correlation for diffusivities in liquids is not as reliable as that for gases. Among several correlations reported, the Wilke-Chang correlation (Wilke and Chang, 1955) is the most widely used for dilute solutions of nonelectrolytes,

$$D_{AB}^{\circ} = \frac{1.173\times10^{-16}(\xi M_B)^{0.5}T}{\mu V_{bA}^{0.6}} \tag{9.4}$$

When the solvent is water, Skelland (1974) recommends the use of the correlation developed by Othmer and Thakar (1953).

$$D_{AB}^{\circ} = \frac{1.112\times10^{-13}}{\mu^{1.1}V_{bA}^{0.6}} \tag{9.5}$$

The preceding two correlations are not dimensionally consistent; therefore, the equations are for use with the units of each term as SI unit as follows:

D°_{AB}	diffusivity of A in B, in a very dilute solution, m2/s
M_B	molecular weight of component B, kg/kmol
T	temperature, °K
μ	solution viscosity, kg/m s
V_{bA}	solute molecular volume at normal boiling point, m^3/kmol 0.0256 m^3/kmol for oxygen [See Perry and Chilton (p.3-233, 1973) for extensive table]
ξ	association factor for the solvent: 2.26 for water, 1.9 for methanol, 1.5 for ethanol, 1.0 for unassociated solvents, such as benzene and ethyl ether.

Example 9.1

Estimate the diffusivity for oxygen in water at 25°C. Compare the predictions from the Wilke-Chang and Othmer-Thakar correlations with the experimental value of 2.5×10^{-9} m^2/s (Perry and Chilton, p. 3-225, 1973). Convert the experimental value to that corresponding to a temperature of 40°C.

Solution:

Oxygen is designated as component A, and water, component B. The molecular volume of oxygen V_{bA} is 0.0256 m^3/kmol. The association factor for water ξ is 2.26. The viscosity of water at 25°C is 8.904×10^{-4} kg/m s (CRC Handbook of Chemistry and Physics , p. F-38, 1983). In Eq. (9.4)

$$D^{\circ}_{AB} = \frac{1.173\times10^{-16}[2.26(18)]^{0.5}298}{(8.904\times10^{-4})^{1.1}(0.0256)^{0.6}} = 2.25\times10^{-9}\,\mathrm{m^2/s}$$

In Eq. (9.5)

$$D^{\circ}_{AB} = \frac{1.112\times10^{-13}}{(8.904\times10^{-4})^{1.1}(0.0256)^{0.6}} = 2.27\times10^{-9}\,\mathrm{m^2/s}$$

If we define the error between these predictions and the experimental value as

$$\% \text{ error} = \frac{\left(D^{\circ}_{AB}\right)_{\text{predicted}} - \left(D^{\circ}_{AB}\right)_{\text{experimental}}}{\left(D^{\circ}_{AB}\right)_{\text{experimental}}} \times 100$$

The resulting errors are –9.6 percent and –9.2 percent for Eqs. (9.4) and (9.5), respectively. Since the estimated possible error for the experimental value is ± 20 percent (Perry and Chilton, p. 3-225, 1973), the estimated values from both equations are satisfactory.

Eq. (9.4) suggests that the quantity $D^{\circ}_{AB}\mu/T$ is constant for a given liquid system. Though this is an approximation, we may use it here to estimate the diffusivity at 40°C. Since the viscosity of water at 40°C is 6.529×10^{-4} kg/m s from the handbook,

$$D^{\circ}_{AB} \text{ at } 40^{\circ}\text{C} = 2.5\times10^{-9}\left(\frac{8.904\times10^{-4}}{6.529\times10^{-4}}\right)\left(\frac{313}{298}\right) = 3.58\times10^{-9}\,\text{m}^2/\text{s}$$

If we use Eq. (9.5), $D^{\circ}_{AB}\mu^{1.1}$ is constant,

$$D^{\circ}_{AB} \text{ at } 40^{\circ}\text{C} = 2.5\times10^{-9}\left(\frac{8.904\times10^{-4}}{6.529\times10^{-4}}\right)^{1.1} = 3.52\times10^{-9}\,\text{m}^2/\text{s}$$

9.2.2. Mass-Transfer Coefficient

The mass flux, the rate of mass transfer q_G per unit area, is proportional to a concentration difference. If a solute transfers from the gas to the liquid phase, its mass flux from the gas phase to the interface N_G is

$$N_G = \frac{q_G}{A} = k_G(C_G - C_{G_i}) \tag{9.6}$$

where C_G and C_{G_i} is the gas-side concentration at the bulk and the interface, respectively, as shown in Figure 9.3. k_G is the individual mass-transfer coefficient for the gas phase and A is the interfacial area.

Similarly, the liquid-side phase mass flux N_L is

$$N_L = \frac{q_L}{A} = k_L(C_{L_i} - C_L) \tag{9.7}$$

where k_L is the individual mass-transfer coefficient for the liquid phase.

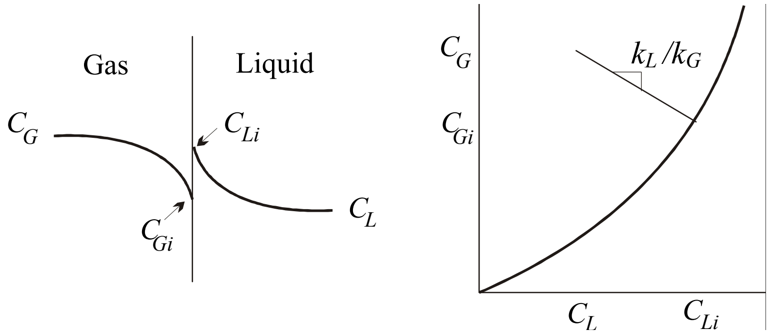

Figure 9.3 Concentration profile near a gas-liquid interface and an equilibrium curve.

Since the amount of solute transferred from the gas phase to the interface must equal that from the interface to the liquid phase,

$$N_G = N_L \tag{9.8}$$

Substitution of Eq. (9.6) and Eq. (9.7) into Eq. (9.8) gives

$$\frac{C_G - C_{G_i}}{C_L - C_{L_i}} = -\frac{k_L}{k_G} \tag{9.9}$$

which is equal to the slope of the curve connecting the (C_L, C_G) and (C_{L_i}, C_{G_i}), as shown in Figure 9.3.

It is hard to determine the mass-transfer coefficient according to Eq. (9.6) or Eq. (9.7) because we cannot measure the interfacial concentrations, C_{L_i} or C_{G_i}. Therefore, it is convenient to define the overall mass-transfer coefficient as follows:

$$N_G = N_L = K_G\left(C_G - C_G^*\right) = K_L\left(C_L^* - C_L\right) \tag{9.10}$$

where C_G^* is the gas-side concentration which would be in equilibrium with the existing liquid phase concentration. Similarly, C_L^* is the liquid-side concentration which would be in equilibrium with the existing gas-phase concentration. These can be easily read from the equilibrium curve as shown in Figure 9.4. The newly defined K_G and K_L are overall mass-transfer coefficients for the gas and liquid sides, respectively.

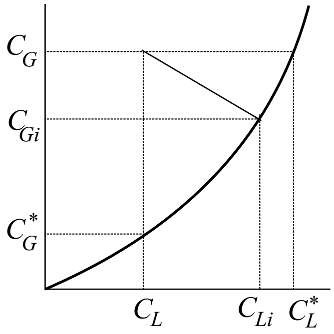

Figure 9.4 The equilibrium curve explaining the meaning of C_G^* and C_L^*

Example 9.2

Derive the relationship between the overall mass-transfer coefficient for liquid phase K_L and the individual mass-transfer coefficients, k_L and k_G. How can this relationship be simplified for sparingly soluble gases?

Solution:

According to Eqs. (9.7) and (9.10),

$$k_L(C_{L_i} - C_L) = K_L\left(C_L^* - C_L\right) \tag{9.11}$$

Therefore, by rearranging Eq. (9.11)

$$\begin{aligned}\frac{1}{K_L} &= \frac{1}{k_L}\frac{C_L^* - C_L}{C_{L_i} - C_L} \\ &= \frac{1}{k_L}\frac{\left(C_{L_i} - C_L\right) + \left(C_L^* - C_{L_i}\right)}{C_{L_i} - C_L} \\ &= \frac{1}{k_L} + \frac{1}{k_L}\frac{\left(C_L^* - C_{L_i}\right)}{C_{L_i} - C_L}\end{aligned} \tag{9.12}$$

Since

$$k_L(C_{L_i} - C_L) = k_G(C_G - C_{G_i}) \tag{9.13}$$

By substituting Eq. (9.13) to Eq. (9.12), we obtain

$$\frac{1}{K_L} = \frac{1}{k_L} + \frac{1}{k_G}\frac{C_L^* - C_L}{C_G - C_{G_i}} = \frac{1}{k_L} + \frac{1}{k_G M} \tag{9.14}$$

which is the relationship between K_L, k_L, and k_G. M is the slope of the line connecting (C_{Li}, C_{Gi}) and (C_L^*, C_G) as shown in Figure 9.4.

For sparingly soluble gases, the slope of the equilibrium curve is very steep; therefore, M is much greater than 1 and from Eq. (9.14)

$$K_L \approx k_L \tag{9.15}$$

Similarly, for the gas-phase mass-transfer coefficient,

$$K_G \approx k_G \tag{9.16}$$

9.2.3. Mechanism of Mass Transfer

Several different mechanisms have been proposed to provide a basis for a theory of interphase mass transfer. The three best known are the two-film theory, the penetration theory, and the surface renewal theory.

The *two-film theory* supposes that the entire resistance to transfer is contained in two fictitious films on either side of the interface, in which transfer occurs by molecular diffusion. This model leads to the conclusion that the mass-transfer coefficient k_L is proportional to the diffusivity D_{AB} and inversely proportional to the film thickness z_f as

$$k_L = \frac{D_{AB}}{z_f} \tag{9.17}$$

Penetration theory (Higbie, 1935)assumes that turbulent eddies travel from the bulk of the phase to the interface where they remain for a constant exposure time t_e. The solute is assumed to penetrate into a given eddy during its stay at the interface by a process of unsteady-state molecular diffusion. This model predicts that the mass-transfer coefficient is directly proportional to the square root of molecular diffusivity

$$k_L = 2\left(\frac{D_{AB}}{\pi t_e}\right)^{1/2} \tag{9.18}$$

Surface renewal theory (Danckwerts, 1951) proposes that there is an infinite range of ages for elements of the surface and the surface age distribution function $\phi(t)$ can be expressed as

$$\phi(t) = se^{-st} \tag{9.19}$$

where s is the fractional rate of surface renewal. This theory predicts that again the mass-transfer coefficient is proportional to the square root of the molecular diffusivity

$$k_L = \left(sD_{AB}\right)^{1/2} \tag{9.20}$$

All these theories require knowledge of one unknown parameter, the effective film thickness z_f, the exposure time t_e, or the fractional rate of surface renewal s. Little is known about these properties, so as theories, all three are incomplete. However, these theories help us to visualize the mechanism of mass transfer at the interface and also to know the exponential dependency of molecular diffusivity on the mass-transfer coefficient.

9.3. Correlation for Mass-Transfer Coefficient

Mass-transfer coefficient is a function of physical properties and vessel geometry. Because of the complexity of hydrodynamics in multiphase mixing, it is difficult, if not impossible, to derive a useful correlation based on a purely theoretical basis. It is common to obtain an empirical correlation for the mass-transfer coefficient by fitting experimental data. The correlations are usually expressed by dimensionless groups since they are dimensionally consistent and also useful for scale-up processes. The dimensionless group important for correlations can be derived by using Buckingham Pi theory as shown in the following example.

Example 9.3

The mass transfer coefficient k_L of oxygen transfer in fermenters is a function of Sauter mean diameter D_{32}, diffusivity D_{AB}, and density ρ_c viscosity μ_c of continuous phase (liquid phase). Sauter-mean diameter D_{32} can be calculated from measured drop-size distribution from the following relationship,

$$D_{32} = \frac{\sum_{i=1}^{n} n_i D_i^3}{\sum_{i=1}^{n} n_i D_i^2} \tag{9.21}$$

Determine appropriate dimensionless parameters that can relate the mass transfer coefficient by applying the Buckingham-Pi theorem.

Solution:

The first step of Buckingham-Pi theorem is to count the total number of parameters. In this case, there are five parameters: k_L, D_{32}, D_{AB}, ρ_c, and μ_c, all of which can be expressed with three principle units: mass M, length L, and time T. Therefore,

Number of parameter: $n = 5$

Number of principle dimension: $r = 3$

In developing the dimensionless groups, every dimensionless group will contain r =3 of repeating parameters and the total number of dimensioness group will be $n - m$ as

Number of repeating parameter: $m = r = 3$

Number of dimensionless group: $n - m = 5 - 3 = 2$

Therefore, we need to choose three repeating parameters. Since we want to develop a correlation for k_L, we want it to be only one dimensionless group and therefore, cannot be a repeating parameter. You can choose any three out of D_{32}, D_{AB}, ρ, and μ, although you may end up different set of dimensionless groups depending on how you select them. If we choose D_{32}, D_{AB}, and ρ as repeating parameters, two dimensionless groups can be constructed as

$$\Pi_1 = D_{32}^a D_{AB}^b \rho_c^c k_L \tag{9.22}$$

$$\Pi_2 = D_{32}^{a'} D_{AB}^{b'} \rho_c^{c'} \mu_c \tag{9.23}$$

Now, the exponents of the above equations can be determined so that both groups can be dimensionless by substituting each parameter with their dimensions as

$$\Pi_1 = \mathrm{L}^a (\mathrm{L}^2/\mathrm{T})^b (\mathrm{M}/\mathrm{L}^3)^c (\mathrm{L}/\mathrm{T}) \tag{9.24}$$

Collecting all exponents for M, T, and L unit,

M: $c = 0$

T: $-b - 1 = 0 \qquad b = -1$

L: $a + 2b - 3c = 0 \qquad a = 1$

Therefore, the first dimensionless group is

$$\Pi_1 = D_{32}^{1} D_{AB}^{-1} \rho_c^{0} k_L = \frac{k_L D_{32}}{D_{AB}} \tag{9.25}$$

which is known as Sherwood number N_{Sh}. Similarly,

$$\Pi_2 = D_{32}^{0} D_{AB}^{-1} \rho_c^{-1} \mu_c = \frac{\mu_c}{D_{AB} \rho_c} \tag{9.26}$$

which is known as Schmidt number, N_{Sc}.

Earlier studies in mass transfer between the gas-liquid phase reported the volumetric mass-transfer coefficient $k_L a$. Since $k_L a$ is the combination of two experimental parameters, mass-transfer coefficient and interfacial area, it is difficult to identify which parameter is responsible for the change of $k_L a$ when we change the operating condition of a fermenter. Calderbank and Moo-Young (1961) separated $k_L a$ by measuring interfacial area and correlated mass-transfer coefficients in gas-liquid dispersions in mixing vessels, and sieve and sintered plate column, as follows:

1. For small bubbles less than 2.5 mm in diameter,

$$k_L = 0.31 N_{Sc}^{-2/3} \left(\frac{\Delta \rho \mu_c g}{\rho_c^{2}} \right)^{1/3} \tag{9.27}$$

or

$$N_{Sh} = 0.31 N_{Sc}^{1/3} N_{Gr}^{1/3} \tag{9.28}$$

where N_{Gr} is known as Grashof number and defined as

$$\text{Grashof number, } N_{Gr} = \frac{D_{32}^{3} \rho_c g \Delta \rho}{\mu_c^{2}} \tag{9.29}$$

The more general forms which can be applied for both small rigid sphere bubble and suspended solid particle are

$$k_L = \frac{2 D_{AB}}{D_{32}} + 0.31 N_{Sc}^{-2/3} \left(\frac{\Delta \rho \mu_c g}{\rho_c^{2}} \right)^{1/3} \tag{9.30}$$

or

$$N_{Sh} = 2.0 + 0.31 N_{Sc}^{1/3} N_{Gr}^{1/3} \tag{9.31}$$

Eqs. (9.30) and (9.31) were confirmed by Calderbank and Jones (1961), for mass transfer to and from dispersions of low-density solid particles in agitated liquids which were designed to simulate mass transfer to microorganisms in fermenters.

2. For bubbles larger than 2.5 mm in diameter,

$$k_L = 0.42 N_{Sc}{}^{-1/2} \left(\frac{\Delta \rho \mu_c g}{\rho_c{}^2} \right)^{1/3} \tag{9.32}$$

or

$$N_{Sh} = 0.42 N_{Sc}{}^{1/2} N_{Gr}{}^{1/3} \tag{9.33}$$

Based on the three theories reviewed in the previous section, the exponential dependency of molecular diffusivity on the mass-transfer coefficient is expected to be some value between 0.5 and 1. It is interesting to note that the exponential dependency of molecular diffusivity in the preceding correlations is 2/3 or 1/2, which is within the range predicted by the theories.

Example 9.4

Estimate the mass-transfer coefficient for the oxygen dissolution in water 25°C in a mixing vessel equipped with flat-blade disk turbine and sparger by using Calderbank and Moo-Young's correlations.

Solution:

The diffusivity of the oxygen in water 25°C is 2.5×10^{-9} m^2/s (Example 9.1). The viscosity and density of water at 25°C is 8.904×10^{-4} kg/m s (*CRC Handbook of Chemistry and Physics*, p. F-38, 1983) and 997.08 kg/m*3* (Perry and Chilton, p. **3**-71, 1973), respectively. The density of air can be calculated from the ideal gas law,

$$\rho_{\text{air}} = \frac{PM}{RT} = \frac{1.01325 \times 10^5 (29)}{8.314 \times 10^3 (298)} = 1.186 \,\text{kg/m}^3$$

Therefore the Schmidt number,

$$N_{Sc} = \frac{\mu}{\rho D_{AB}} = \frac{8.904 \times 10^{-4}}{997.08(2.5 \times 10^9)} = 357.2$$

Substituting in Eq. (9.27) for small bubbles,

$$k_L = 0.31(357.2)^{-2/3}\left[\frac{(997.08-1.186)(8.904\times10^{-4})(9.81)}{(997.08)^2}\right]^{1/3}$$
$$= 1.27\times10^{-4}\ \text{m/s}$$

Substituting in Eq. (9.32) for large bubbles,

$$k_L = 0.42(357.2)^{-1/2}\left[\frac{(997.08-1.186)(8.904\times10^{-4})(9.81)}{(997.08)^2}\right]^{1/3}$$
$$= 4.58\times10^{-4}\ \text{m/s}$$

Therefore, for the air-water system, Eqs. (9.27) and (9.32) predict that the mass-transfer coefficients for small and large bubbles are 1.27×10^{-4} and 4.58×10^{-4} m/s, respectively, which are independent of power consumption and gas-flow rate.

Eq. (9.32) predicts that the the mass-transfer coefficient for the oxygen dissolution in water 25°C in a mixing vessel is 4.58×10^{-4} m/s, regardless of the power consumption and gas-flow rate as illustrated in the previous example problem. Lopes De Figueiredo and Calderbank (1978) reported later that the value of k_L varies from 7.3×10^{-4} to 3.4×10^{-3} m/s, depending on the power dissipation by impeller per unit volume ($P_{m/v}$) as

$$k_L \propto \left(\frac{P_m}{v}\right)^{0.33} \tag{9.34}$$

This dependence of k_L on P_m/v was also reported by Prasher and Wills (1973) based on the absorption of CO_2 into water in an agitated vessel, as follows:

$$k_L = 0.592 D_{AB}^{1/2}\left(\frac{P_m}{v\mu_c}\right)^{0.25} \tag{9.35}$$

which is dimensionally consistent. However, this equation is limited in its use because the correlation is based on only one gas-liquid system.

Akita and Yoshida (1974) evaluated the liquid-phase mass-transfer coefficient based on the oxygen absorption into several liquids of different physical properties using bubble columns without mechanical agitation. Their correlation for k_L is

$$\frac{k_L D_{32}}{D_{AB}} = 0.5\left(\frac{\nu_c}{D_{AB}}\right)^{1/2}\left(\frac{gD_{32}{}^{3}}{\nu_c{}^{2}}\right)^{1/4}\left(\frac{gD_{32}{}^{2}\rho_c}{\sigma}\right)^{3/8} \tag{9.36}$$

where ν_c and σ are the kinematic viscosity of the continuous phase and interfacial tension, respectively. Eq. (9.36) is applicable for column diameters of up to 0.6 m, superficial gas velocities up to 25 m/s, and gas hold-ups to 30 percent.

9.4. Measurement of Interfacial Area

To calculate the gas absorption rate q_L for Eq. (9.7), we need to know the gas-liquid interfacial area, which can be measured employing several techniques such as photography, light transmission, and laser optics.

The interfacial area per unit volume can be calculated from the Sauter-mean diameter D_{32} and the volume fraction of gas-phase H, as follows:

$$a = \frac{6H}{D_{32}} \tag{9.37}$$

The Sauter-mean diameter, a surface-volume mean, can be calculated by measuring drop sizes directly from photographs of a dispersion according to Eq. (9.21).

Photographic measurement of drop sizes is the most straightforward method among many techniques because it does not require calibration. However, taking a clear picture may be difficult, and reading the picture is tedious and time consuming. Pictures can be taken through the base or the sidewall of a mixing vessel. To eliminate the distortion due to the curved surface of a vessel wall, the vessel can be immersed in a rectangular tank, or a water pocket can be installed on the wall (Skelland and Lee, 1981). One limitation of this approach is that the measurement of drop size is limited to the regions near the wall, which may not represent the overall dispersion in a fermenter. Another method is to take pictures by immersing the extension tube with a objective lense in the tank as described by Hong and Lee (1983).

Drop size distribution can be indirectly measured by using the light-transmission technique. When a beam of light is passed through a gas-liquid dispersion, light is scattered by the gas bubbles. It was found that a plot of the extinction ratio (reciprocal of light transmittance, *1/T*) against interfacial area per unit volume of dispersion *a*, gave a straight line, as follows (Vermeulen et al., 1955; Calderbank, 1958):

$$\frac{1}{T} = m_1 + m_2 a \tag{9.38}$$

In theory, m_1 is unity and m_2 is a constant independent of drop-size distribution as long as all the bubbles are approximately spherical.

The light transmission technique is most frequently used for the determination of average bubble size in gas-liquid dispersion. It has the advantages of quick measurement and on-line operation. The probes are usually made of mirror-treated glass rods (Vermeulen et al., 1955), internally blackened tubes with mirrors (Calderbank, 1958), or fiber optic light guide (Hong and Lee, 1983).

9.5. Correlations for *a* and *D₃₂*

9.5.1. Gas Sparging with No Mechanical Agitation

Leaving the vicinity of a sparger, the bubbles may break up or coalesce with others until an equilibrium size distribution is reached. A stable size is achieved when turbulent fluctuations and surface tension forces are in balance (Calderbank, 1959).

Akita and Yoshida (1974) determined the bubble-size distribution in bubble columns using a photographic technique. The gas was sparged through perforated plates and single orifices, while various liquids were used. The following correlation was proposed for the Sauter-mean diameter:

$$\frac{D_{32}}{D_C} = 26\left(\frac{g\,D_C^2\rho_c}{\sigma}\right)^{-0.5}\left(\frac{gD_C^3}{\nu_c^2}\right)^{-0.12}\left(\frac{V_s}{\sqrt{gD_C}}\right)^{-0.12} \tag{9.39}$$

and for the interfacial area

$$aD_C = \frac{1}{3}\left(\frac{g\,D_C^2\rho_L}{\sigma}\right)^{0.5}\left(\frac{gD_C^3}{\nu_L^2}\right)^{0.1} H^{1.13} \tag{9.40}$$

where D_C is bubble column diameter and V_s is superfical gas velocity, which is gas flow rate Q divided by the tank cross-sectional area. Eqs. (9.39) and (9.40) are based on data in columns of up to 0.3 m in diameter and up to superficial gas velocities of about 0.07 m/s.

9.5.2. Gas Sparging with Mechanical Agitation

Calderbank (1958) correlated the interfacial areas for the gas-liquid dispersion agitated by a flat-blade disk turbine as follows:

1. For $V_s < 0.02$ m/s,

$$a_0 = 1.44\left[\frac{(P_m/v)^{0.4}\rho_c^{\ 0.2}}{\sigma^{0.6}}\right]\left(\frac{V_s}{V_t}\right)^{1/2} \tag{9.41}$$

for

$$N_{\mathrm{Re}_i}^{0.7}\left(\frac{ND_I}{V_s}\right)^{0.3} < 20{,}000$$

where N_{Re_i} is the impeller Reynolds number defined as

$$N_{\mathrm{Re}_i} = \frac{D_I^2 N\rho_c}{\mu_c} \tag{9.42}$$

The interfacial area for $N_{\mathrm{Re}_i}^{0.7}\left(ND_I/V_s\right)^{0.3} > 20{,}000$ can be calculated from the interfacial area a_0 obtained from Eq. (9.41) by using the following relationship.

$$\log_{10}\left(\frac{2.3a}{a_0}\right) = \left(1.95\times10^{-5}\right)N_{\mathrm{Re}_i}^{0.7}\left(\frac{ND_I}{V_s}\right)^{0.3} \tag{9.43}$$

2. For $V_s > 0.02$ m/s, Miller (1974) modified Eq. (9.41) by replacing the aerated power input by mechanical agitation P_m with the effective power input P_e, and the terminal velocity V_t with the sum of the superficial gas velocity and the terminal velocity $V_s + V_t$. The effective power input P_e combines both gas sparging and mechanical agitation energy contributions. The modified equation is

$$a_0 = 1.44\left[\frac{(P_e/v)^{0.4}\rho_c^{\ 0.2}}{\sigma^{0.6}}\right]\left(\frac{V_s}{V_t + V_s}\right)^{1/2} \tag{9.44}$$

Calderbank (1958) also correlated the Sauter-mean diameter for the gas-liquid dispersion agitated by a flat-blade disk turbine impeller as follows:

1. For dispersion of air in pure water,

$$D_{32} = 4.15\left[\frac{\sigma^{0.6}}{(P_m/v)^{0.4}\rho_c^{\ 0.2}}\right]H^{0.5} + 9.0\times10^{-4} \tag{9.45}$$

2. In electrolyte solutions (NaCl, Na_2SO_4, and Na_3PO_4),

$$D_{32} = 2.25\left[\frac{\sigma^{0.6}}{(P_m/v)^{0.4}\,\rho_c^{\,0.2}}\right]H^{0.4}\left(\frac{\mu_d}{\mu_c}\right)^{0.25} \tag{9.46}$$

3. In alcoholic solution (aliphatic alcohols),

$$D_{32} = 1.90\left[\frac{\sigma^{0.6}}{(P_m/v)^{0.4}\,\rho_c^{\,0.2}}\right]H^{0.65}\left(\frac{\mu_d}{\mu_c}\right)^{0.25} \tag{9.47}$$

where all constants are dimensionless except 9.0×10^{-4} m in Eq. (9.45). Again the preceding three equations can be modified for high gas flow rate ($V_s > 0.02$ m/s) by replacing P_m by P_e, as suggested by Miller (1974).

9.6. Gas Hold-Up

Gas hold-up is one of the most important parameters characterizing the hydrodynamics in a fermenter. Gas hold-up depends mainly on the superficial gas velocity and the power consumption, and often is very sensitive to the physical properties of the liquid. Gas hold-up can be determined easily by measuring level of the aerated liquid during operation Z_F and that of clear liquid Z_L. Thus, the average fractional gas hold-up H is given as

$$H = \frac{Z_F - Z_L}{Z_F} \tag{9.48}$$

Gas Sparging with No Mechanical Agitation: In a two-phase system where the continuous phase remains in place, the hold-up is related to superficial gas velocity V_s and bubble rise velocity V_t (Sridhar and Potter, 1980):

$$H = \frac{V_s}{V_s + V_t} \tag{9.49}$$

Akita and Yoshida (1973) correlated the gas hold-up for the absorption of oxygen in various aqueous solutions in bubble columns, as follows:

$$\frac{H}{(1-H)^4} = 0.20\left(\frac{g\,D_C^2\rho_c}{\sigma}\right)^{1/8}\left(\frac{gD_C^3}{v_c^2}\right)^{1/12}\left(\frac{V_s}{\sqrt{gD_C}}\right) \tag{9.50}$$

Gas Sparging with Mechanical Agitation: Calderbank (1958) correlated gas hold-up for the gas-liquid dispersion agitated by a flat-blade disk turbine impeller as

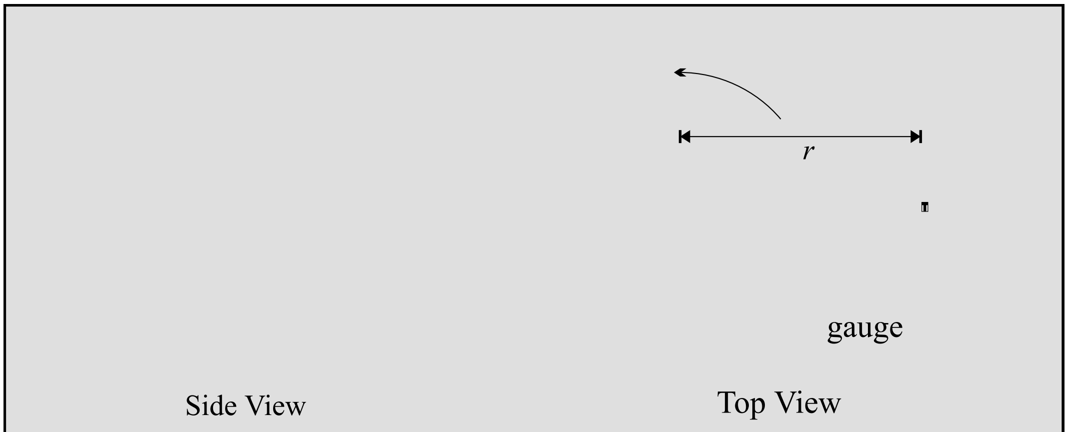

Figure 9.5 A torque table to measure the power consumption for mechanical agitation.

$$H = \left(\frac{V_s H}{V_t}\right)^{1/2} + (2.16\times10^{-4})\left[\frac{(P_m/v)^{0.4}\,\rho_c^{\,0.2}}{\sigma^{0.6}}\right]\left(\frac{V_s}{V_t}\right)^{1/2} \tag{9.51}$$

where 2.16×10^{-4} has a unit (m) and $V_t = 0.265$ m/s when the bubble size is in the range of 2–5 mm diameter. The preceding equation can be obtained by combining Eqs. (9.41) and Eq. (9.45) by means of Eq. (9.37).

For high superficial gas velocities ($V_s > 0.02$ m/s), replace P_m and V_t of Eq. (9.51) with effective power input P_e and $V_t + V_s$, respectively (Miller, 1974).

9.7. Power Consumption

The power consumption for mechanical agitation can be measured using a torque table as shown in Figure 9.5. The torque table is constructed by placing a thrust bearing between a base and a circular plate, and the force required to prevent rotation of the turntable during agitation F is measured. The power consumption P can be calculated by the following formula

$$P = 2\pi rNF \tag{9.52}$$

where N is the agitation speed, and r is the distance from the axis to the point of the force measurement.

Power consumption by agitation is a function of physical properties, operating condition, and vessel and impeller geometry. Dimensional analysis provides the following relationship:

$$\frac{P}{\rho N^3 D_I^{\;5}} = f\left(\frac{\rho N D_I^{\;2}}{\mu}, \frac{N^2 D_I}{g}, \frac{D_T}{D_I}, \frac{H}{D_I}, \frac{D_W}{D_I}, \ldots\right) \tag{9.53}$$

The dimensionless group in the left-hand side of Eq. (9.53) is known as power number N_P, which is the ratio of drag force on impeller to inertial force. The first term of the right-hand side of Eq. (9.53) is the impeller Reynolds number N_{Re_i}, which is the ratio of inertial force to viscous force, and the second term is the Froude number N_{Fr}, which takes into account gravity forces. The gravity force affects the power consumption due to the formation of the vortex in an agitating vessel. The vortex formation can be prevented by installing baffles.

For fully baffled geometrically similar systems, the effect of the Froude number on the power consumption is negligible and all the length ratios in Eq. (9.53) are constant. Therefore, Eq. (9.53) is simplified to

$$N_P = \alpha\left(N_{Re}\right)^{\beta} \tag{9.54}$$

Figure 9.6 shows Power number-Reynolds number correlation in an agitator with four baffles (Rushton et al., 1950) for three different types of impellers. The power number decreases with an increase of the Reynolds number and reaches a constant value when the Reynolds number is larger than 10,000. At this point, the power number is independent of the Reynolds number. For the normal operating condition of gas-liquid contact, the Reynolds number is usually larger than 10,000. For example, for a 3-inch impeller with an agitation speed of 150 rpm, the impeller Reynolds number is 16,225 when the liquid is water. Therefore, Eq. (9.54) is simplified to

$$N_p = \text{constant} \qquad \text{for} \quad N_{Re} > 10{,}000 \tag{9.55}$$

The power required by an impeller in a gas sparged system P_m is usually less than the power required by the impeller operating at the same speed in a gas-free liquids P_{mo}. The P_m for the flat-blade disk turbine can be calculated from P_{mo} (Nagata, 1975), as follows:

$$\log_{10}\frac{P_m}{P_{mo}} = -192\left(\frac{D_I}{D_T}\right)^{4.38}\left(\frac{D_I^{\;2} N}{\nu}\right)^{0.115}\left(\frac{D_I N^2}{g}\right)^{1.96\left(\frac{D_I}{D_T}\right)}\left(\frac{Q}{N D_I^{\;3}}\right) \tag{9.56}$$

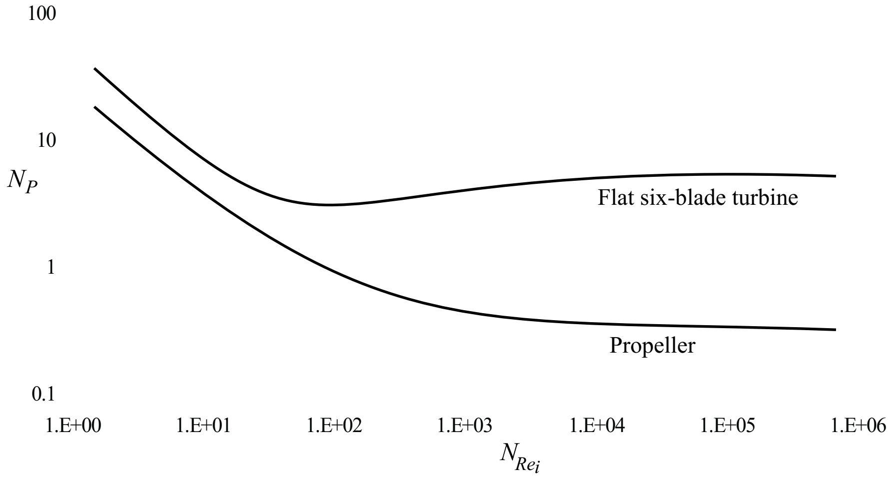

Figure 9.6 Power number–Reynolds number correlation in an agitator with four baffles (each $0.1D_T$). (Rushton, et al., 1950)

Example 9.5

A cylindrical tank (1.22 m diameter) is filled with water to an operating level equal to the tank diameter. The tank is equipped with four equally spaced baffles whose width is one tenth of the tank diameter. The tank is agitated with a 0.36 m diameter flat six-blade disk turbine. The impeller rotational speed is 2.8 rps. The air enters through an open-ended tube situated below the impeller and its volumetric flow rate is 0.00416 m 3/s at 1.08 atm and 25°C.

Calculate the following properties and compare the calculated values with those experimental data reported by Chandrasekharan and Calderbank (1981): $P_m = 697$ W; $H = 0.02$; $k_La = 0.0217$ s^{-1}.

a. Power requirement

b. Gas hold-up

c. Sauter-mean diameter

d. Interfacial area

e. Volumetric mass-transfer coefficient

Solution:

a. Power requirement: The viscosity and density of water at 25°C is 8.904×10^{-4} kg/m s (CRC Handbook of Chemistry and Physics , p.

F-38, 1983) and 997.08 kg/m^3 (Perry and Chilton, p. **3**-71, 1973), respectively. Therefore, the Reynolds number is

$$N_{Re} = \frac{\rho N D_I^2}{\mu} = \frac{(997.08)(2.8)(0.36)^2}{8.904 \times 10^{-4}} = 406{,}357$$

which is much larger than 10,000, above which the power number is constant at 6. Thus,

$$P_{mo} = 6\rho N^3 D_I^5 = 6(997.08)(2.8)^3(0.36)^5 = 794\,\mathrm{W}$$

The power required in the gas-sparged system is from Eq. (9.56)

$$\log_{10}\frac{P_m}{P_{mo}} = -192\left(\frac{0.36}{1.22}\right)^{4.38}\left(\frac{0.36^2(2.8)}{8.93\times 10^{-7}}\right)^{0.115}\left(\frac{(0.36)2.8^2}{9.81}\right)^{1.96\left(\frac{0.36}{1.22}\right)}\left(\frac{0.00416}{(2.8)0.36^3}\right)$$

Therefore,

$$P_m = 687\,\mathrm{W}$$

b. Gas hold-up: The interfacial tension for the air-water interface is 0.07197 kg/s^2 (CRC Handbook of Chemistry and Physics , p. F-33, 1983). The volume of the the dispersion is

$$v = \frac{\pi}{4}1.22^2(1.22) = 1.43\,\mathrm{m}^3$$

The superficial gas velocity is

$$V_s = \frac{4Q}{\pi DT^2} = \frac{4(0.00416)}{\pi 1.22^2} = 0.00356\,\mathrm{m/s}$$

Substituting these values into Eq. (9.51) gives

$$H = \left(\frac{0.00356H}{0.265}\right)^{1/2} + 2.16\times 10^{-4}\left[\frac{(687/1.43)^{0.4}997.08^{0.2}}{0.07197^{0.6}}\right]\left(\frac{0.00356}{0.265}\right)^{1/2}$$

The solution of the preceding equation for H gives

$$H = 0.023$$

c. Sauter-mean diameter: In Eq. (9.45)

$$D_{32}=4.15\left[\frac{0.07197^{0.6}}{(687/1.43)^{0.4}997.08^{0.2}}\right]0.023^{0.5}+9.0\times10^{-4}$$
$$=0.00366\,\mathrm{m}=3.9\,\mathrm{mm}$$

d. Interfacial area a: In Eq. (9.37)

$$a=\frac{6H}{D_{32}}=\frac{6\ (0.023)}{0.00366}=37.7\,\mathrm{m}^{-1}$$

e. Volumetric mass-transfer coefficient: Since the average size of bubbles is 4 mm, we should use Eq. (9.32) . Then, from Example 9.4

$$k_L=4.58\times10^{-4}\ \mathrm{m/s}$$

Therefore,

$$k_La=4.58\times10^{-4}(37.7)=0.017\,\mathrm{s}^{-1}$$

The preceding estimated values compare well with those experimental values. The percent errors as defined in Example 9.1 are –1.4 percent for the power consumption, 15 percent for the gas hold-up, and –21.7 percent for the volumetric mass-transfer coefficient.

9.8. Determination of Oxygen-Absorption Rate

To estimate the design parameters for oxygen uptake in a fermenter, you can use the correlations presented in the previous sections, which can be applicable to a wide range of gas-liquid systems in addition to the air-water system. However, the calculation procedure is lengthy and the predicted value from those correlations can vary widely. Sometimes, you may be unable to find suitable correlations which will be applicable to your type and size of fermenters. In such cases, you can measure the oxygen-transfer rate yourself or use correlations based on those experiments.

The oxygen absorption rate per unit volume q_a/v can be estimated by

$$\frac{q_a}{v}=K_La(C_L^{\ *}-C_L)=k_La(C_L^{\ *}-C_L) \tag{9.57}$$

Since the oxygen is sparingly soluble gas, the overall mass-transfer coefficient K_L is equal to the individual mass-transfer coefficient k_L. Our objective in fermenter design is to maximize the oxygen transfer rate with the minimum power consumption necessary to agitate the fluid, and also

Table 9.1

Solubility of Oxygen in Water at 1 atm.[a]

Temperature	Solubility	
°C	mmol O_2/L	mg O_2/L
0	2.18	69.8
10	1.70	54.5
15	1.54	49.3
20	1.38	44.2
25	1.26	40.3
30	1.16	37.1
35	1.09	34.9
40	1.03	33.0

[a] Data from International Critical Tables, Vol. III, New York: McGraw-Hill Book Co., 1928, p. 271.

minimum air flow rate. To maximize the oxygen absorption rate, we have to maximize k_L, a, $C_L^* - C_L$. However, the concentration difference is quite limited for us to control because the value of C_L^* is limited by its very low maximum solubility. Therefore, the main parameters of interest in design are the mass-transfer coefficient and the interfacial area.

Table 9.1 lists the solubility of oxygen at 1 atm in water at various temperatures. The value is the maximum concentration of oxygen in water when it is in equilibrium with pure oxygen. This solubility decreases with the addition of acid or salt as shown in Table 9.2.

Normally, we use air to supply the oxygen demand of fermenters. The maximum concentration of oxygen in water which is in equilibrium with air C_L^* at atmospheric pressure is about one fifth of the solubility listed, according to the Henry's law,

$$C_L^* = \frac{p_{O_2}}{H_{O_2}(T)} \tag{9.58}$$

where p_{O_2} is the partial pressure of oxygen and $H_{O_2}(T)$ is Henry's law constant of oxygen at a temperature, T. The value of Henry's law constant can be obtained from the solubilities listed in Table 9.2. For example, at 25°C, C_L^*

Table 9.2
Solubility of Oxygen in Solution of Salt or Acid at 25°C.[a]

Conc.	Solubility, mmol O_2/L		
mol/L	HCl	H_2SO_4	NaCl
0.0	1.26	1.26	1.26
0.5	1.21	1.21	1.07
1.0	1.16	1.12	0.89
2.0	1.12	1.02	0.71

[a] Data from F. Todt, Electrochemishe Sauer-stoffmessungen, Berlin: W. de Guy & Co., 1958.

is 1.26 mmol/L and p_{O_2} is 1 atm because it is pure oxygen. By substituting these values into Eq. (9.58), we obtain $H_{O_2}(25^\circ\text{C})$ is 0.793 atm L/mmol. Therefore, the equilibrium concentration of oxygen for the air-water contact at 25°C will be

$$C_L^* = \frac{0.209\ \text{atm}}{0.793\ \text{atm L/mmol}} = 0.264\ \text{mmol}\ \text{O}_2\,/\,\text{L} = 8.43\ \text{mg/L}$$

Ideally, oxygen-transfer rates should be measured in a fermenter which contains the nutrient broth and microorganisms during the actual fermentation process. However, it is difficult to carry out such a task due to the complicated nature of the medium and the ever changing rheology during cell growth. A common strategy is to use a synthetic system which approximates fermentation conditions.

9.8.1. Sodium Sulfite Oxidation Method

The sodium sulfite oxidation method (Cooper et al., 1944) is based on the oxidation of sodium sulfite to sodium sulfate in the presence of catalyst (Cu^{++} or Co^{++}) as

$$\text{Na}_2\text{SO}_3 + \frac{1}{2}\text{O}_2 \xrightarrow{\text{Cu}^{++}\text{ or Co}^{++}} \text{Na}_2\text{SO}_4 \tag{9.59}$$

This reaction has following characteristics to be qualified for the measurement of the oxygen-transfer rate:

1. The rate of this reaction is independent of the concentration of sodium sulfite within the range of 0.04 to 1 N.
2. The rate of reaction is much faster than the oxygen transfer rate; therefore, the rate of oxidation is controlled by the rate of mass transfer alone.

To measure the oxygen-transfer rate in a fermenter, fill the fermenter with a 1 N sodium sulfite solution containing at least 0.003 M Cu^{++} ion. Turn on the air and start a timer when the first bubbles of air emerge from the sparger. Allow the oxidation to continue for 4 to 20 minutes, after which, stop the air stream, agitator, and timer at the same instant, and take a sample. Mix each sample with an excess of freshly pipetted standard iodine reagent. Titrate with standard sodium thiosulfate solution ($Na_2S_2O_3$) to a starch indicator end point. Once the oxygen uptake is measured, the k_L a may be calculated by using Eq. (9.57) where C_L is zero and C_L^* is the oxygen equilibrium concentration.

The sodium sulfite oxidation technique has its limitation in the fact that the solution cannot approximate the physical and chemical properties of a fermentation broth. An additional problem is that this technique requires high ionic concentrations (1 to 2 mol/L), the presence of which can affect the interfacial area and, in a lesser degree, the mass-transfer coefficient (Van't Riet, 1979). However, this technique is helpful in comparing the performance of fermenters and studying the effect of scale-up and operating conditions.

Example 9.6

To measure k_L a, a fermenter was filled with 10 L of 0.5 M sodium sulfite solution containing 0.003 M Cu^{++} ion and the air sparger was turned on. After exactly 10 minutes, the air flow was stopped and a 10 mL sample was taken and titrated. The concentration of the sodium sulfite in the sample was found to be 0.21 mol/L. The experiment was carried out at 25°C and 1 atm. Calculate the oxygen uptake and k_La.

Solution:

The amount of sodium sulfite reacted for 10 minutes is

$$0.5 - 0.21 = 0.29 \text{ mol/L}$$

According to the stoichiometric relation, Eq. (9.59) the amount of oxygen required to react 0.29 mol/L is

$$0.29^{12} = 0.145\,\text{mol/L}$$

Therefore, the oxygen uptake is

$$(0.145\,\text{mole O}_2/L)\left(\frac{32\,\text{g O}_2/\text{mol}}{600\,\text{s}}\right) = 7.73\times10^{-3}\ \text{g/Ls}$$

The solubility of oxygen in equilibrium with air can be estimated by Eq. (9.58) as

$$C_L^* = \frac{p_{\text{O}_2}}{H_{\text{O}_2}(T)} = \frac{(1\,\text{atm})(0.209\,\text{mol O}_2/\text{mol air})}{(793\,\text{atm L/mol})(1\,\text{mol}/32\,\text{g})} = 8.43\times10^{-4}\ \text{g/L}$$

Therefore, the value of $k_L a$ is, according to the Eq. (9.57),

$$k_L a = \frac{q_a / v}{C_L^* - C_L} = \frac{7.73\times10^{-3}\,\text{g/Ls}}{(8.43\times10^{-3}\,\text{g/L} - 0)} = 0.917\ \text{s}^{-1}$$

9.8.2. Dynamic Gassing-out Technique

This technique (Van't Riet, 1979) monitors the change of the oxygen concentration while an oxygen-rich liquid is deoxygenated by passing nitrogen through it. Polarographic electrode is usually used to measure the concentration. The mass balance in a vessel gives

$$\frac{dC_L(t)}{dt} = k_L a\ [C_L^* - C_L(t)] \tag{9.60}$$

Integration of the preceding equation between t_1 and t_2 results in

$$k_L a = \frac{\ln\left[\dfrac{C_L^* - C_L(t_1)}{C_L^* - C_L(t_2)}\right]}{t_2 - t_1} \tag{9.61}$$

from which $k_L a$ can be calculated based on the measured values of $C_L(t_1)$ and $C_L(t_2)$.

9.8.3. Direct Measurement

In this technique, we directly measure the oxygen content of the gas stream entering and leaving the fermenter by using gaseous oxygen analyzer. The oxygen uptake can be calculated as

$$q_a = (Q_{\text{in}} C_{\text{O}_2,\text{in}} - Q_{\text{out}} C_{\text{O}_2,\text{out}}) \tag{9.62}$$

where Q is the gas flow rate.

Once the oxygen uptake is measured, the k_L a can be calculated by using Eq. (9.57), where C_L is the oxygen concentration of the liquid in a fermenter and C_L^* is the concentration of the oxygen which would be in equilibrium with the gas stream. The oxygen concentration of the liquid in a fermenter can be measured by an on-line oxygen sensor. If the size of the fermenter is rather small (less than 50 L), the variation of the $C_L^* - C_L$ in the fermenter is fairly small. However, if the size of a fermenter is very large, the variation can be significant. In this case, the log-mean value of $C_L^* - C_L$ of the inlet and outlet of the gas stream can be used as

$$\left(C_L^* - C_L\right)_{LM} = \frac{\left(C_L^* - C_L\right)_{in} - \left(C_L^* - C_L\right)_{out}}{\ln\left[\left(C_L^* - C_L\right)_{in} / \left(C_L^* - C_L\right)_{out}\right]} \tag{9.63}$$

9.8.4. Dynamic Technique

By using the dynamic technique (Taguchi and Humphrey, 1966), we can estimate the $k_L a$ value for the oxygen transfer during an actual fermentation process with real culture medium and microorganisms. This technique is based on the oxygen material balance in an aerated batch fermenter while microorganisms are actively growing as

$$\frac{dC_L}{dt} = k_L a(C_L^{\,*} - C_L) - r_{\text{O}_2} C_X \tag{9.64}$$

where r_{O_2} is cell respiration rate [g O_2/g cell h].

While the dissolved oxygen level of the fermenter is steady, if you suddenly turn off the air supply, the oxygen concentration will be decreased (Figure 9.7) with the following rate

$$\frac{dC_L}{dt} = r_{\text{O}_2} C_X \tag{9.65}$$

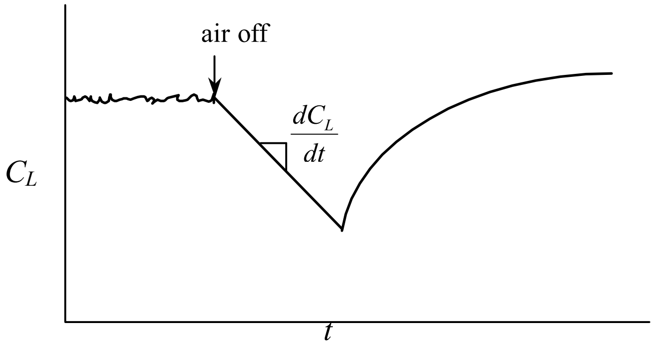

Figure 9.7 Dynamic technique for the determination of k_La.

since k_La in Eq. (9.64) is equal to zero. Therefore, by measuring the slope of the C_L vs. t curve, we can estimate $r_{O_2}C_X$. If you turn on the airflow again, the dissolved oxygen concentration will be increased according to Eq. (9.64), which can be rearranged to result in a linear relationship as

$$C_L = C_L^* - \frac{1}{k_La}\left(\frac{dC_L}{dt} + r_{O_2}C_X\right) \tag{9.66}$$

The plot of C_L versus $dC_L/dt + r_{O_2}C_X$ will result in a straight line which has the slope of $-1/(k_La)$ and the y-intercept of C_L^*.

9.9. Correlation for k_La

9.9.1. Bubble Column

Akita and Yoshida (1973) correlated the volumetric mass-transfer coefficient k_La for the absorption of oxygen in various aqueous solutions in bubble columns, as follows:

$$k_La = 0.6 D_{AB}^{0.5} \nu_c^{-0.12} \left(\frac{\sigma}{\rho_c}\right)^{-0.62} D_T^{0.17} g^{0.93} H^{1.1} \tag{9.67}$$

which applies to columns with less effective spargers.

In bubble columns, for $0 < V_s < 0.15$ m/s and $100 < P_g/v < 1100$ W/m^3, Botton et al. (1980) correlated the k_La as

$$\frac{k_La}{0.08} = \left(\frac{P_g/v}{800}\right)^{0.75} \tag{9.68}$$

where P_g is the gas power input, which can be calculated from

$$\frac{p_g}{v} = 800\left(\frac{V_s}{0.1}\right)^{0.75} \tag{9.69}$$

9.9.2. Mechanically Agitated Vessel

For aerated mixing vessels in an aqueous solution, the mass-transfer coefficient is proportional to the power consumption (Lopes De Figueiredo and Calderbank, 1978) as

$$k_L \propto \left(\frac{P_m}{v}\right)^{0.33} \tag{9.70}$$

The interfacial area for the aerated mixing vessel is a function of agitation conditions. Therefore, according to Eq. (9.41),

$$a \propto \left(\frac{P_m}{v}\right)^{0.4} V_s^{0.5} \tag{9.71}$$

Therefore, by combining the above two equations, $k_L a$ will be

$$k_L a \propto \left(\frac{P_m}{v}\right)^{0.77} V_s^{0.5} \tag{9.72}$$

Numerous studies for the correlations of $k_L a$ have been reported and their results have the general form as

$$k_L a = b_1\left(\frac{P_m}{v}\right)^{b_2} V_s^{b_3} \tag{9.73}$$

where b_1, b_1, and b_1 vary considerably depending on the geometry of the system, the range of variables covered, and the experimental method used. The values of b_2 and b_3 are generally between 0 to 1 and 0.43 to 0.95, respectively, as tabulated by Sideman et al. (1966).

Van't Riet (1979) reviewed the data obtained by various investigators and correlated them as follows:

1. For "coalescing" air-water dispersion,

$$k_L a = 0.026\left(\frac{P_m}{v}\right)^{0.4} V_s^{0.5} \tag{9.74}$$

1. For “noncoalescing” air-electrolyte solution dispersions,

$$k_L a = 0.002\left(\frac{P_m}{v}\right)^{0.7} V_s^{\,0.2} \qquad (9.75)$$

both of which are applicable for the volume up to 2.6 m^3; for a wide variety of agitator types, sizes, and D_I/D_T ratios; and $500 < P_{m/v} < 10{,}000$ W/m^3. These correlations are accurate within approximately 20 percent to 40 percent.

Example 9.7

Estimate the volumetric mass-transfer coefficient $k_L a$ for the gas-liquid contactor described in Example 9.4 by using the correlation for $k_L a$ in this section.

Solution:

From Example 9.4, the reactor volume v is 1.43 m^3, the superficial gas velocity V_s is 0.00356 m/s, and power consumption P_m is 687 W. By substituting these values into Eq. (9.74),

$$k_L a = 0.026\left(\frac{687}{1.43}\right)^{0.4} 0.00356^{0.5} = 0.018\,\mathrm{s}^{-1}$$

9.10. Scale-Up

9.10.1. Similitude

For the optimum design of a production-scale fermentation system (prototype), we must translate the data on a small scale (model) to the large scale. The fundamental requirement for scale-up is that the model and prototype should be similar to each other.

Two kinds of conditions must be satisfied to insure similarity between model and prototype. They are:

1. Geometric similarity of the physical boundaries: The model and the prototype must be the same shape, and all linear dimensions of the model must be related to the corresponding dimensions of the prototype by a constant scale factor.

2. Dynamic similarity of the flow fields: The ratio of flow velocities of corresponding fluid particles is the same in model and prototype as well as the ratio of all forces acting on corresponding fluid particles. When dynamic similarity of two flow fields with geometrically similar boundaries is achieved, the flow fields exhibit geometrically similar flow patterns.

The first requirement is obvious and easy to accomplish, but the second is difficult to understand and also to accomplish and needs explanation. For example, if forces that may act on a fluid element in a fermenter during agitation are the viscosity force F_V, drag force on impeller F_D, and gravity force F_G, each can be expressed with characteristic quantities associated with the agitating system. According to Newton's equation of viscosity, viscosity force is

$$F_V = \mu \left(\frac{du}{dy} \right) A \tag{9.76}$$

where *du/dy* is velocity gradient and A is the area on which the viscosity force acts. For the agitating system, the fluid dynamics involved are too complex to calculate a wide range of velocity gradients present. However, it can be assumed that the average velocity gradient is proportional to agitation speed *N* and the area *A* is to D_I^2, which results.

$$F_V \propto \mu N D_I^2 \tag{9.77}$$

The drag force F_D can be characterized in an agitating system as

$$F_D \propto \frac{P_{mo}}{D_I N} \tag{9.78}$$

Since gravity force F_G is equal to mass m times gravity constant *g*,

$$F_G \propto \rho D_I^3 g \tag{9.79}$$

The summation of all forces is equal to the inertial force F_I as,

$$\sum F = F_V + F_D + F_G = F_I \propto \rho D_I^4 N^2 \tag{9.80}$$

Then dynamic similarity between a model (*m*) and a prototype (*p*) is achieved if

$$\frac{(F_V)_m}{(F_V)_p} = \frac{(F_D)_m}{(F_D)_p} = \frac{(F_G)_m}{(F_G)_p} = \frac{(F_I)_m}{(F_I)_p} \tag{9.81}$$

or in dimensionless forms:

$$\left(\frac{F_I}{F_V}\right)_p=\left(\frac{F_I}{F_V}\right)_m$$

$$\left(\frac{F_I}{F_D}\right)_p=\left(\frac{F_I}{F_D}\right)_m \tag{9.82}$$

$$\left(\frac{F_I}{F_G}\right)_p=\left(\frac{F_I}{F_G}\right)_m$$

The ratio of inertial force to viscosity force is

$$\frac{F_I}{F_V}=\frac{\rho {D_I}^4N^2}{\mu N{D_I}^2}=\frac{\rho {D_I}^2N}{\mu}=N_{\mathrm{Re}_i} \tag{9.83}$$

which is the Reynolds number. Similarly,

$$\frac{F_I}{F_V}=\frac{\rho {D_I}^4N^2}{P_{mo}/D_IN}=\frac{\rho N^3{D_I}^5}{P_{mo}}=\frac{1}{N_P} \tag{9.84}$$

$$\frac{F_I}{F_G}=\frac{\rho {D_I}^4N^2}{\rho {D_I}^3g}=\frac{D_IN^2}{g}=N_{Fr} \tag{9.85}$$

Dynamic similarity is achieved when the values of the nondimensional parameters are the same at geometrically similar locations.

$$(N_{\mathrm{Re}_i})_p=(N_{\mathrm{Re}_i})_m$$

$$(N_P)_p=(N_P)_m \tag{9.86}$$

$$(N_{Fr})_p=(N_{Fr})_m$$

Therefore, using dimensionless parameters for the correlation of data has advantages not only for the consistency of units, but also for the scale-up purposes.

However, it is difficult, if not impossible, to satisfy the dynamic similarity when more than one dimensionless group is involved in a system, which creates the needs of scale-up criteria. The following example addresses this problem.

Example 9.8

The power consumption by an agitator in an unbaffled vessel can be expressed as

$$\frac{P}{\rho N^3 D_I^{\,5}} = f\left(\frac{\rho N D_I^{\,2}}{\mu}, \frac{N^2 D_I}{g}\right)$$

Can you determine the power consumption and impeller speed of a 1,000-gallon fermenter based on the findings of the optimum condition from a geometrically similar one-gallon vessel? If you cannot, can you scale up by using a different fluid system?

Solution:

Since V_p / V_m = 1,000, the scale ratio is,

$$\frac{(D_I)_p}{(D_I)_m} = 1{,}000^{1/3} = 10 \tag{9.87}$$

To achieve dynamic similarity, the three dimensionless numbers for the prototype and the model must be equal, as follows:

$$\left(\frac{P_{mo}}{\rho N^3 D_I^{\,5}}\right)_p = \left(\frac{P_{mo}}{\rho N^3 D_I^{\,5}}\right)_m \tag{9.88}$$

$$\left(\frac{\rho N D_I^{\,2}}{\mu}\right)_p = \left(\frac{\rho N D_I^{\,2}}{\mu}\right)_m \tag{9.89}$$

$$\left(\frac{N^2 D_I}{g}\right)_p = \left(\frac{N^2 D_I}{g}\right)_m \tag{9.90}$$

If you use the same fluid for the model and the prototype, $\rho_p = \rho_m$ and $\mu_p = \mu_m$. Canceling out the same physical properties and substituting Eq. (9.87) to Eq. (9.88) yields

$$(P_{mo})_p = 10^5 (P_{mo})_m \left(\frac{N_p}{N_m}\right)^3 \tag{9.91}$$

The equality of the Reynolds number requires

$$N_p = 0.01\, N_m \tag{9.92}$$

On the other hand, the equality of the Froude number requires

$$N_p = \frac{1}{\sqrt{10}} N_m \tag{9.93}$$

which is conflicting with the previous requirement for the equality of the Reynolds number. Therefore, it is impossible to satisfy the requirement of the dynamic similarity unless you use different fluid systems.

If $\rho_p \neq \rho_m$ and $\mu_p \neq \mu_m$, to satisfy Eqs. (9.89) and (9. 90), the following relationship must hold.

$$\left(\frac{\mu}{\rho}\right)_m = \frac{1}{31.6}\left(\frac{\mu}{\rho}\right)_p \tag{9.94}$$

Therefore, if the kinematic viscosity of the prototype is similar to that of water, the kinematic viscosity of the fluid, which needs to be employed for the model, should be 1/31.6 of the kinematic viscosity of water. It is impossible to find the fluid whose kinematic viscosity is that small. As a conclusion, if all three dimensionless groups are important, it is impossible to satisfy the dynamic similarity.

The previous example problem illustrates the difficulties involved in the scale-up of the findings of small-scale results. Therefore, we need to reduce the number of dimensionless parameters involved to as few as possible, and we also need to determine which is the most important parameter, so that we may set this parameter constant. However, even though only one dimensionless parameter may be involved, we may need to define the scale-up criteria.

As an example, for a fully baffled vessel when $N_{Re_i} > 10{,}000$, the power number is constant according to Eq. (9.55). For a geometrically similar vessel, the dynamic similarity will be satisfied by

$$\left(\frac{P_{mo}}{\rho N^3 D_I^{\,5}}\right)_p = \left(\frac{P_{mo}}{\rho N^3 D_I^{\,5}}\right)_m \tag{9.95}$$

If the fluid employed for the prototype and the model remains the same, the power consumption in the prototype is

$$\left(P_{mo}\right)_p = \left(P_{mo}\right)_m \left(\frac{N_p}{N_m}\right)^3 \left[\frac{\left(D_I\right)_m}{\left(D_I\right)_p}\right]^5 \tag{9.96}$$

where $(D_I)_p/(D_I)_m$ is equal to the scale ratio. With a known scale ratio and known operating conditions of a model, we are still unable to predict the operating conditions of a prototype because there are two unknown variables, P_{mo} and N. Therefore, we need to have a certain criteria which can be used as a basis.

9.10.2. Criteria of Scale-Up

Most often, power consumption per unit volume P_{mo}/v is employed as a criterion for scale-up. In this case, to satisfy the equality of power numbers of a model and a prototype,

$$\left(\frac{P_{mo}}{D_I^3}\right)_p = \left(\frac{P_{mo}}{D_I^3}\right)_m \left(\frac{N_p}{N_m}\right)^3 \left[\frac{(D_I)_p}{(D_I)_m}\right]^2 \tag{9.97}$$

Note that P_{mo}/D_I^3 represents the power per volume because the liquid volume is proportional to D_I^3 for the geometrically similar vessels. For the constant P_{mo}/D_I^3,

$$\left(\frac{N_p}{N_m}\right)^3 = \left[\frac{(D_I)_m}{(D_I)_p}\right]^2 \tag{9.98}$$

As a result, if we consider scale-up from a 20-gallon to a 2,500-gallon agitated vessel, the scale ratio is equal to 5, and the impeller speed of the prototype will be

$$N_p = \left[\frac{(D_I)_m}{(D_I)_p}\right]^{2/3} N_m = 0.34 N_m \tag{9.99}$$

which shows that the impeller speed in a prototype vessel is about one third of that in a model. For constant P_{mo}/v, the Reynolds number and the impeller tip speed cannot be the same. For the scale ratio of 5,

$$(N_{\mathrm{Re}_i})_p = 8.5(N_{\mathrm{Re}_i})_m \tag{9.100}$$

$$(ND_I)_p = 1.7(ND_I)_m \tag{9.101}$$

Table 9.3
Properties of Agitator on Scale-Up[a]

Property	Model 20 gal	Prototype 2,500 gal			
P_{mo}	1.0	125.	3126	25	0.2
P_{mo}/v	1.0	**1.0**	25	0.2	0.0016
N	1.0	0.34	1.0	0.2	0.04
D_I	1.0	5.0	5.0	5.0	5.0
Q	1.0	42.5	125	25	5.0
Q/v	1.0	0.34	**1.0**	0.2	0.04
ND_I	1.0	1.7	5.0	**1.0**	0.2
N_{Re}	1.0	8.5	25	5.0	**1.0**

[a] Reprinted with permission from J. Y. Oldshue, "Mixing Scale-Up Techniques" *Biotech. Bioeng.* 8 (1966):3–24. ©1966 by John Wiley & Sons, Inc., New York, NY.

Table 9.3 shows the values of properties for a prototype (2,500-gallon) when those for a model (20-gallon) are arbitrarily set as 1.0 (Oldshue, 1966). The parameter values of the prototype depend on the criteria used for the scale-up. The third column shows the parameter values of the prototype, when P_{mo}/v is set constant. The values in the third column seem to be more reasonable than those in the fourth, fifth, and sixth columns, which are calculated based on the constant value of Q/v, ND_I, and $ND_I^2\rho/\mu$, respectively. For example when the Reynolds number is set constant for the two scales, the P_{mo}/v reduces to 0.16 percent of the model and actual power consumption P_{mo} also reduces to 20 percent of the model, which is totally unreasonable.

As a conclusion, there is no one scale-up rule that applies to many different kinds of mixing operations. Theoretically we can scale up based on geometrical and dynamic similarities, but it has been shown that it is possible for only a few limited cases. However, some principles for the scale-up are as follows (Oldshue, 1985):

1. It is important to identify which properties are important for the optimum operation of a mixing system. This can be mass transfer, pumping capacity, shear rate, or others. Once the important properties are identified, the system can be scaled up so that those properties can

be maintained, which may result in the variation of the less important variables including the geometrical similarity.

2. The major differences between a big tank and a small tank are that the big tank has a longer blend time, a higher maximum impeller shear rate, and a lower average impeller shear rate.
3. For homogeneous chemical reactions, the power per volume can be used as a scale-up criterion. As a rule of thumb, the intensity of agitation can be classified based on the power input per 1,000 gallon as shown in Table 9.4

Table 9.4
Criteria of Agitation Intensity

Horsepower per 1000 gal	Agitation Intensity
0.5 – 1	Mild
2 – 3	Vigorous
4 – 10	Intense

4. For the scale-up of the gas-liquid contactor, the volumetric mass-transfer coefficient kLa can be used as a scale-up criterion. In general, the volumetric mass-transfer coefficient is approximately correlated to the power per volume. Therefore, constant power per volume can mean a constant kLa.
5. Typical impeller-to-tank diameter ratio D_I/T for fermenters is 0.33 to 0.44. By using a large impeller, adequate mixing can be provided at an agitation speed which does not damage living organisms. Fermenters are not usually operated for an optimum gas-liquid mass transfer because of the shear sensitivity of cells, which is discussed in the next section.

9.11. Shear-Sensitive Mixing

One of the most versatile fermenter systems used industrially is the mechanically agitated fermenter. This type of system is effective in the mixing of fermenter contents, the suspension of cells, the breakup of air bubbles for enhanced oxygenation, and the prevention of forming large cell aggregates. However, the shear generated by the agitator can disrupt the cell membrane and eventually kill some microorganisms (Midler and Fin, 1966), animal cells (Croughan et al., 1987), and plant cells (Hooker et al., 1988). Shear also is responsible for the deactivation of enzymes (Charm and Wong, 1970). As a result, for optimum operation of an agitated fermentation system, we need to understand the hydrodynamics involved in shear sensitive mixing.

For the laminar flow region of Newtonian fluid, shear stress τ is equal to the viscosity μ times the velocity gradient du/dy as

$$\tau = -\mu \frac{du}{dy} \tag{9.102}$$

which is known as Newton's equation of viscosity. The velocity gradient is also known as shear rate .

For the turbulent flow,

$$\tau = -\eta \frac{du}{dy} \tag{9.103}$$

where η is eddy viscosity, which is not only dependent upon the physical properties of the fluid, but also the operating conditions. Therefore, to describe the intensity of shear in a turbulent system such as an agitated fermenter, it is easier to estimate shear rate du/dy instead of shear stress.[1] Even though we use the shear rate as a measure of the shear intensity, we should remember that it is the shear stress that ultimately affects the living cells or enzyme. Depending upon the magnitude of viscosity and also whether the flow is laminar or turbulent, there is a wide range of shear stress generated for the same shear rate. However, the shear rate is a good measure for the intensity of the agitation.

In agitated systems, it is difficult, if not impossible, to determine the shear rate, because of the complicated nature of the fluid dynamics generated by impellers. A fluid element in an agitated vessel will go through a wide range of shear rates during agitation: maximum shear when it passes through the impeller region and minimum shear when it passes near the corner of the vessel. Metzner and Otto (1957) developed a general correlation for the average shear rate generated by a flat-blade disk turbine, based on power measurements on non-Newtonian liquids, as:

---

[1] For a non-Newtonian fluid, the viscosity is not constant even for the laminar flow. Therefore, shear rate is easier to estimate than shear stress.

$$\left(-\frac{du}{dy}\right)_{av} = 13N \qquad \text{for} \quad N_{Re_i} < 20 \tag{9.104}$$

9.12. Nomenclature

A	interfacial area, m^2
a	gas-liquid interfacial area per unit volume of dispersion for low impeller Reynolds numbers, m^{-1}
a_0	gas-liquid interfacial area per unit volume of dispersion, m^{-1}
b	constant
C	concentration, kmol/ m^3
C_D	friction factor and drag coefficient, dimensionless D diameter of bubble or solid particle, m
D_{AB}	diffusivity of component A through B, m^2/s
D°_{AB}	diffusivity of component A in a very dilute solution of B, m^2/s
D_{32}	Sauter-mean diameter, m
D_I	impeller diameter, m
D_T	tank diameter, m
D_W	impeller width, m
F	force, N
J_A	molar flux of component A relative to the average molal velocity of all constituents, kmol/ m^{2}s
K	overall mass-transfer coefficient, m/s
k	individual mass-transfer coefficient, m/s
g	acceleration due to gravity, m/s^2
H	volume fraction of gas phase in dispersion, dimensionless
N	impeller speed, s -1
N_A, N_B	mass flux of A and B relative to stationary coordinate, kmol/ m^{2}s
N_{Fr}	Froude number (D_IN^2/g),dimensionless
N_G, N_L	mass flux from gas to liquid phase and from liquid to gas phase, respectively, kmol/m^{2}s
N_{Gr}	Grashof number ($D_{32}^3\rho_c\Delta\rho g/\mu_c^2$), dimensionless
N_o	number of sparger orifices or sites

N_P	power number ($P_{mo} / \rho D_I^5 N^3$), dimensionless
N_{Re_b}	bubble Reynolds number ($D_{BM} V_t \rho_c / \mu_c$), dimensionless
N_{Re_i}	impeller Reynolds number ($D_I^2 N \rho_c / \mu_c$), dimensionless
N_{Sc}	Schmidt number ($\mu_c / \rho_c D_{AB}$), dimensionless
N_{Sh}	Sherwood number ($k_L D_{32} / D_{AB}$), dimensionless
P	total pressure, N/m^2
P_e	effective power input by both gas sparging and mechanical agitation, W
P_g	power dissipated by sparged gas, W
P_m	power dissipated by impeller in aerated liquid dispersion, W
P_{mo}	power dissipated by impeller without aeration, W
q	the rate of mass transfer, kmol/s
Q	volumetric gas-flow rate, m^3/s
R	gas constant
r	length of radial arm for dynamometer system, m
s	fractional rate of surface renewal, s^{-1}
t_e	exposure time for the penetration theory, s
u	velocity, m/s
u_o	sparger hole velocity, m/s
V_s	superficial gas velocity, gas-flow rate divided by tank cross sectional area, m/s
V_t	terminal gas-bubble velocity in free rise, m/s
v	volume of liquid, m^3
Z_F, Z_L	level of the aerated liquid during operation, and that of clear liquid, m
z_f	film thickness in the two-film theory, m
η	0.06, fraction of jet energy transmitted to bulk liquid
$\Delta\rho$	difference in density between dispersed (gas) and continuous (liquid) phases, kg/m 3
γ	shear rate, s^{-1}
μ	viscosity, kg/m s
ν	kinematic viscosity, m^2/s
ω	angular velocity, s^{-1}

π	absolute pressure, N/ m^2
π_o	pressure at sparger, N/ m^2
ρ	density, kg/m 3
ϕ(t)	surface age distribution function
σ	surface tension, kg/s^2
τ	shear stress, N/ m^2

SUBSCRIPT

c	continuous phase or liquid phase
d	dispersed phase or gas phase
G	gas phase
g	gas phase
L	liquid phase

9.13. Problems

9.1 Derive the relationship between the overall mass transfer coefficient for gas phase K_G and the individual mass-transfer coefficients, k_L and k_G. How can this relationship be simplified for sparingly soluble gases?

9.2 Prove that Eq. (9.27) is the same with Eq. (9.28), and Eq. (9.30) is the same with Eq. (9.31).

9.3 The power consumption by impeller P in geometrically similar fermenters is a function of the diameter D_I and speed N of impeller, density ρ and viscosity μ of liquid, and acceleration due to gravity g. Determine appropriate dimensionless parameters that can relate the power consumption by applying dimensional analysis using the Buckingham-Pi theorem.

9.4 A cylindrical tank (1.22 m diameter) is filled with water to an operating level equal to the tank diameter. The tank is equipped with four equally spaced baffles, the width of which is one tenth of the tank diameter. The tank is agitated with a 0.36 m diameter, flat-blade disk turbine. The impeller rotational speed is 4.43 rps. The air enters through an open-ended tube situated below the impeller and its volumetric flow rate is 0.0217 m^3/s at 1.08 atm and 25°C. Calculate:

a. power requirement
b. gas hold-up
c. Sauter-mean diameter
d. interfacial area
e. volumetric mass-transfer coefficient

Compare the preceding calculated results with those experimental values reported by Chandrasekharan and Calderbank (1981): P_m = 2282 W; $H = 0.086$; $k_L a = 0.0823$ s^{-1}.

9.5 Estimate the volumetric mass-transfer coefficient k_L a for the gas-liquid contactor described in Problem 9.4 by using a correlation for k_L a and compare the result with the experimental value.

9.6 The power consumption by an agitator in an unbaffled vessel can be expressed as

$$\frac{P_{mo}}{\rho N^3 D_I^{\ 5}} = f\left(\frac{\rho N D_I^{\ 2}}{\mu}\right)$$

Can you determine the power consumption and impeller speed of a 1,000-gallon fermenter based on findings of the optimum condition from a one-gallon vessel by using the same fluid system? Is your conclusion reasonable? Why or why not?

9.7 The optimum agitation speed for the cultivation of plant cells in a 3-L fermenter equipped with four baffles was found to be 150 rpm.

a. What should be the impeller speed of a geometrically similar 1,000 L fermenter if you scale up based on the same power consumption per unit volume.

b. When the impeller speed suggested by part (a) was employed for the cultivation of a 1,000-L fermenter, the cells do not seem to grow well due to the high shear generated by the impeller even though the impeller speed is lower than 150 rpm of the model system. This may be due to the higher impeller tip speed which is proportional to ND_I. Is this true? Justify your answer with the ratio of the impeller tip speed of the prototype to the model fermenter.

c. If you use the impeller tip speed as the criteria for the scale-up, what will be the impeller speed of the prototype fermenter?

9.8 The typical oxygen demand for yeast cells growing on hydrocarbon is about 3 g per g of dry cell. Design a 10-L stirred fermenter (the diameter and height of fermenter, the type and diameter of impeller) and determine its operating condition (impeller speed and aeration rate) in order to meet the oxygen demand during the peak growth period with the growth rate of 0.5 g dry cell per liter per hour. You can assume that the physical properties of the medium is the same as pure water. You are free to make additional assumptions in order to design the required fermenter.

9.14. References

Akita, K. and F. Yoshida, "Gas Holdup and Volumetric Mass Transfer Coefficient in Bubble Column," *I&EC Proc. Des. Dev.* **12** (1973):76–80.

Akita, K. and F. Yoshida, "Bubble Size, Interfacial Area, and Liquid-Phase Mass Transfer Coefficient in Bubble Columns," *I&EC Proc. Des. Dev.* **13** (1974):84–91.

Botton, R., D. Cosserat, and J. C. Charpentier, "Operating Zone and Scale Up of Mechanically Stirred Gas-Liquid Reactors," *Chem. Eng. Sci.* **35** (1980):82–89.

Bowen, R. L., "Unraveling the Mysteries of Shear-sensitive Mixing Systems," *Chem. Eng.* **9** (1986):55–63.

Calderbank, P. H., "Physical Rate Processes in Industrial Fermentation, Part I: Interfacial Area in Gas-Liquid Contacting with Mechanical Agitation," *Trans. Instn. Chem. Engrs.* **36** (1958):443–459.

Calderbank, P. H., "Physical Rate Processes in Industrial Fermentation, Part II: Mass Transfer Coefficients in Gas-Liquid Contacting with and without Mechanical Agitation," *Trans. Instn. Chem. Engrs.* **37** (1959):173–185.

Calderbank, P. H. and S. J. R. Jones, "Physical Rate Properties in Industrial Fermentation – Part III. Mass Transfer from Fluids to Solid Particles Suspended in Mixing Vessels," *Trans. Instn. Chem. Engrs.* **39** (1961):363–368.

Calderbank, P. H. and M. B. Moo-Young, "The Continuous Phase Heat and Mass-Transfer Properties of Dispersions," *Chem. Eng. Sci.* **16** (1961):39–54.

Chandrasekharan, K. and P. H. Calderbank, "Further Observations on the Scale-up of Aerated Mixing Vessels," *Chem. Eng. Sci.* **36** (1981):819–823.

Charm, S. E. and B. L. Wong, "Enzyme Inactivation with Shearing," *Biotechnol. Bioeng.* **12** (1970):1103–1109.

Cooper, C. M., G. A. Fernstrom, and S. A. Miller, "Performance of Agitated Gas-Liquid Contactors," *Ind. Eng. Chem.* **36** (1944):504–509.

Croughan, M. S., J.-F. Hamel, and D. I. C. Wang, "Hydrodynamic Effects on Animal Cells Grown in Microcarrier Cultures," *Biotech. Bioeng.* **29** (1987):130–141.

CRC Handbook of Chemistry and Physics. Cleveland, OH: CRC Press, 1983.

Danckwerts, P. V., "Significance of Liquid-Film Coefficients in Gas Absorption," *Ind. Eng. Chem.* **43** (1951):1460–1467.

Higbie, R. "The rate of absorption of a pure gas into a still liquid during short periods of exposure," *Trans. AIChE* **31** (1935):365–389.

Hong, P. O. and J. M. Lee, "Unsteady-State Liquid-Liquid Dispersions in Agitated Vessels," *I&EC Proc. Des. Dev.* **22** (1983):130–135.

Hooker, B. S., J. M. Lee, and G. An, "The Response of Plant Tissue Culture to a High Shear Environment," *Enzyme Microb. Technol.* **11** (1989):484–490.

Lopes De Figueiredo, M. M. and P. H. Calderbank, "The Scale-Up of Aerated Mixing Vessels for Specified Oxygen Dissolution Rates," *Chem. Eng. Sci.* **34** (1979):1333–1338.

Metzner, A. B. and R. E. Otto, "Agitation of Non-Newtonian Fluids," *AIChE J.* **3** (1957):3–10.

Midler, Jr., M. and R. K. Finn, "A Model System for Evaluating Shear in the Design of Stirred Fermentors," *Biotech. Bioeng.* **8** (1966):71–84.

Miller, D. N., "Scale-Up of Agitated Vessels Gas-Liquid Mass Transfer," *AIChE J.* **20** (1974):442–453.

Nagata, S., *Mixing: Principles and Application,* pp. 59–62. New York, NY: John Wiley & Sons, 1975.

Oldshue, J. Y., "Fermentation Mixing Scale-Up Techniques," *Biotech. Bioeng.* **8** (1966):3–24.

Oldshue, J. Y., "Current Trends in Mixer Scale-up Techniques," in *Mixing of Liquids by Mechanical Agitation* , ed. J. J. Ulbrecht and G. K. Patterson. New York: Gordon and Breach Science Publishers, 1985, pp. 309–342.

Othmer, D. F. and M. S. Thakar, "Correlating Diffusion Coefficients in Liquids," *Ind. Eng. Chem.* **45** (1953):589–593.

Perry, R. H. and C. H. Chilton, *Chemical Engineers' Handbook,* (5th ed.). New York, NY: McGraw-Hill Book Co., 1973.

Prasher, B. D. and G. B. Wills, "Mass Transfer in an Agitated Vessel," *I&EC Proc. Des. Dev.* **12** (1973):351–354.

Rushton, J. H., E. W. Costich, and H. J. Everett, "Power Characteristics of Mixing Impellers, Part II," *Chem. Eng. Prog.* **46** (1950):467–476.

Sideman, S., O. Hortacsu, and J. W. Fulton, "Mass Transfer in Gas-Liquid Contacting System," *Ind. Eng. Chem.* **58** (1966):32–47.

Skelland, A. H. P., *Diffusional Mass Transfer*, pp. 56–58. New York, NY: John Wiley & Sons, 1974.

Skelland, A. H. P. and J. M. Lee, "Drop Size and Continuous Phase Mass Transfer in Agitated Vessels," *AIChE J.* **27** (1981):99–111.

Sridhar, T. and O. E. Potter, "Gas Holdup and Bubble Diameters in Pressurized Gas-Liquid Stirred Vessels," *I & E. C. Fundam.* **19** (1980):21–26.

Taguchi, H. and A. E. Humphrey, "Dynamic Measurement of Volumetric Oxygen Transfer Coefficient in Fermentation Systems," *J. Ferment. Tech.*(Jap.) **44** (1966):881–889.

Van't Riet, K., "Review of Measuring Methods and Results in Nonviscous Gas-Liquid Mass Transfer in Stirred Vessels," *I&EC Proc. Des. Dev.* **18** (1979):357–364.

Vermeulen, T., G. M. Williams, and G. E. Langlois, "Interfacial Area in Liquid-Liquid and Gas-Liquid Agitation," *Chem. Eng. Prog.* **51** (1955):85F–94F.

Wilke, C. R. and P. Chang, "Correlation of Diffusion Coefficients in Dilute Solutions," *AIChE J.* **1** (1955):264–270.